HAL open science

Smolyak Algorithm Adapted to a System–Bath Separation:Application to an Encapsulated Molecule with Large-AmplitudeMotions

Chen Ahai, David Benoit, Yohann Scribano, André Nauts, David Lauvergnat

▶ **To cite this version:**

Chen Ahai, David Benoit, Yohann Scribano, André Nauts, David Lauvergnat. Smolyak Algorithm Adapted to a System–Bath Separation:Application to an Encapsulated Molecule with Large-AmplitudeMotions. Journal of Chemical Theory and Computation, 2022, 18 (7), pp.4366-4372. 10.1021/acs.jctc.2c00108 . hal-03723977

HAL Id: hal-03723977

https://hal.science/hal-03723977v1

Submitted on 31 Oct 2022

HAL is a multi-disciplinary open access archive for the deposit and dissemination of scientific research documents, whether they are published or not. The documents may come from teaching and research institutions in France or abroad, or from public or private research centers.

L'archive ouverte pluridisciplinaire **HAL**, est destinée au dépôt et à la diffusion de documents scientifiques de niveau recherche, publiés ou non, émanant des établissements d'enseignement et de recherche français ou étrangers, des laboratoires publics ou privés.

arXiv:2201.05857v3 [physics.atom-ph] 27 Apr 2022

A Smolyak algorithm adapted to a system-bath separation: application to an encapsulated molecule with large amplitude motions

Ahai Chen,[†,‡] David M. Benoit ,[¶] Yohann Scribano,[§] André Nauts,[‖,‡] and David Lauvergnat[*,‡]

†*Université Paris-Saclay, UVSQ, CNRS, CEA, Maison de la Simulation, 91191, Gif-sur-Yvette, France*

‡*Université Paris-Saclay, CNRS, Institut de Chimie Physique, UMR-CNRS 8000, 91405 Orsay, France*

¶*E.A. Milne Centre for Astrophysics, The University of Hull, Cottingham Road, Kingston upon Hull HU6 7RX, UK*

§*Laboratoire Univers et Particules de Montpellier, Université de Montpellier, UMR-CNRS 5299, 34095 Montpellier Cedex, France*

‖*Institute of Condensed Matter and Nanosciences (NAPS), Université Catholique de Louvain, Louvain-la-Neuve, Belgium*

E-mail: david.lauvergnat@universite-paris-saclay.fr

Abstract

A Smolyak algorithm adapted to system-bath separation is proposed for rigorous quantum simulations. This technique combines a sparse grid method with the system-

bath concept in a specific configuration without limitations on the form of the Hamiltonian, thus achieving a highly efficient convergence of the excitation transitions for the “system" part. Our approach provides a general way to overcome the perennial convergence problem for the standard Smolyak algorithm and enables the simulation of floppy molecules with more than a hundred degrees of freedom. The efficiency of the present method is illustrated on the simulation of H_2 caged in an sII clathrate hydrate including two kinds of cage modes. The transition energies are converged by increasing the number of normal modes of water molecules. Our results confirm the triplet splittings of both translational and rotational ($j = 1$) transitions of the H_2 molecule. Furthermore, they show a slight increase of the translational transitions with respect to the ones in a rigid cage.

1 Introduction

The study of quantum systems coupled to a complex host, for instance, the guest-host complexes,[1–4] has attracted strong interest in recent years,[5–7] spanning the fields of fundamental quantum physics, physical chemistry, quantum optics, etc. Some of these problems go beyond a structureless environment description, leading to the emergence of more accurate non-Markovian quantum models based on a system-bath approach.[6–8] Given the well-known exponential scaling of the problem, the bath is usually described using effective approaches, e.g. a collection of harmonic oscillators, with a reconstructed effective system-bath coupling, e.g. the spectral density formulation.[6,9–11] These approaches are limited, to some extent, to specifically tailored systems. Meanwhile, a variety of multi-configurational quantum dynamics method have been proposed, for example the well-known multi-configuration time-dependent Hartree (MCTDH) method,[12,13] the variational multi-configurational Gaussian (vMCG) method[14] and their extended versions.[4,15] These methods have been shown to be highly efficient, although MCTDH normally requires a sum-of-product expression for the potentials to cover specific problems.

The Smolyak method[16–18] has been used as an accurate and efficient tensor compression method for high-dimensional grids and applied successfully to obtain the vibrational spectra of molecules up to 12 degrees of freedom (DoF).[19–28] At present, the approach is capable of treating a few tens of DoF, opening up a new direction for the improvement of quantum dynamics simulation.[19,21–23,25,26] This method provides a way of selecting simultaneously basis functions and an associated sparse grid. So the number of basis functions and grid points will not scale exponentially with the system dimension. The Smolyak algorithm can be naturally embedded in a system-bath model (see Eq.(1)-Eq.(4) below) to simulate a molecule or part of a molecule surrounded by a complex environment. The approach has no limitation on the formulation of the Hamiltonian and does not require the reconstruction of bath mode and system-bath coupling. However, we show here that converging the transition energies between system levels without converging the bath levels is rather difficult in the standard Smolyak scheme.

In this work, we propose a new Smolyak algorithm adapted to a system-bath separation (SSBS) to overcome this problem (see Fig.1). To illustrate this method, we study a single H_2 molecule caged in a clathrate hydrate. A hydrogen clathrate hydrate is a typical host-guest system and is considered a promising hydrogen-storage candidate for future clean energy.[29–31] The dynamics of the caged H_2 molecule is sensitive to the environment and highly quantum mechanical. A benchmark experiment[32] has confirmed the triplet splittings of both translational fundamental and rotational (j=1) transitions (T,R) of H_2 induced by the cage anisotropy.[33] However, investigating this system with full cage dynamics is challenging. We use SSBS to enable the simulation of the TR transitions for more than a hundred DoF. Our approach is tested using two different sets of cage normal modes (NM) to validate the method.

2 Method

In conventional quantum simulations, the wave function is expanded in primitive basis sets $B^i \equiv \{|b^i_1\rangle, |b^i_2\rangle, \cdots, |b^i_{N^{b^i}}\rangle\}$ ($i\in[1,n]$) as a full direct-product:

$$|\Psi\rangle = \sum_{k_1=1}^{N^{b^1}} \cdots \sum_{k_n=1}^{N^{b^n}} C^{\boldsymbol{B}}_{\boldsymbol{k}} |b^1_{k_1}\rangle |b^2_{k_2}\rangle \cdots |b^n_{k_n}\rangle, \tag{1}$$

where $\boldsymbol{k}\equiv\{k_1, k_2, \cdots, k_n\}$, $\boldsymbol{B}\equiv\{B^1, B^2, \cdots, B^n\}$ and $C^{\boldsymbol{B}}_{\boldsymbol{k}}$ is the coefficient of the wave function expansion associated with the basis function, $|b^1_{k_1}\rangle|b^2_{k_2}\rangle\cdots|b^n_{k_n}\rangle$. N^{b^i} is the size of the B^i basis set.

In the Smolyak method, the wave function is expressed instead as:

$$|\Psi\rangle \;=\; \sum_{\mathscr{R}(\boldsymbol{\ell})} D_{\boldsymbol{\ell}} |\psi^{\boldsymbol{\ell}}\rangle. \tag{2}$$

The Smolyak term, $|\psi^{\boldsymbol{\ell}}\rangle$, is projected on restricted basis sets $B^i_\ell \equiv \{|b^i_1\rangle, |b^i_2\rangle, \cdots, |b^i_{N^{b^i}_{\ell_i}}\rangle\}$,

$$|\psi^{\boldsymbol{\ell}}\rangle = \sum_{k_1=1}^{N^{b^1}_{\ell_1}} ... \sum_{k_n=1}^{N^{b^n}_{\ell_n}} C^{\boldsymbol{B}_{\boldsymbol{\ell}}}_{\boldsymbol{k}} |b^1_{k_1}\rangle |b^2_{k_2}\rangle \cdots |b^n_{k_n}\rangle, \tag{3}$$

as a small direct-product with respect to the usual full one (Eq.(1)), where $\boldsymbol{B}_{\boldsymbol{\ell}} \equiv \{B^1_{\ell_1}, B^2_{\ell_2}, \cdots, B^n_{\ell_n}\}$, $\boldsymbol{\ell} \equiv \{\ell_1, \ell_2, \cdots, \ell_n\}$. $N^{b_i}_{\ell_i}$ is the size of the restricted basis B^i_ℓ, defined as an arbitrarily increasing integer sequence function of ℓ_i.[20,24,34] Usually, it is chosen as $A_i+B_i\ell_i$ ($A_i\geq 0$, $B_i\geq 1$, $A_i, B_i\in\mathbb{Z}$). The sum in Eq.(2) is restricted to specific Smolyak terms through the constraint, $\mathscr{R}(\boldsymbol{\ell})$: L-n+1$\leq|\boldsymbol{\ell}|\leq L$, where $|\boldsymbol{\ell}|=\sum_{i=1}^n \ell_i$. The coefficient $D_{\boldsymbol{\ell}}$ is defined as $(-1)^{L-|\boldsymbol{\ell}|}\binom{n-1}{L-|\boldsymbol{\ell}|}$, where $\binom{n-1}{L-|\boldsymbol{\ell}|}$ is a binomial coefficient. The Smolyak parameter, L (or L^B), is a constant that controls the approximation level for the nD-basis set and therefore its size. The total number of basis functions required is now reduced to $N^s_L=\sum_{\mathscr{R}(\boldsymbol{\ell})}(\prod_{i=1}^n N^{b^i}_{\ell_i})$. In terms of the tensor products in the Smolyak scheme,[16,23] the full nD-space can be represented

as:

$$S_L = \sum_{\mathscr{R}(\boldsymbol{\ell})} D_{\boldsymbol{\ell}} \cdot S^1_{\ell_1} \otimes S^2_{\ell_2} \otimes \cdots \otimes S^n_{\ell_n}, \tag{4}$$

where $S^i_{\ell_i}$ ($i \in [1, n]$) can be the restricted basis sets B^i_ℓ or grids $\{Q^i_1, Q^i_2, \cdots, Q^i_{N^{q^i}_{\ell_i}}\}$ and $N^{q_i}_{\ell_i}$ (the number of gaussian quadrature grid points) is defined similarly to $N^{b_i}_{\ell_i}$. This feature enables ones to define a unique Smolyak scheme simultaneously for the basis set and the grid, giving a sparse grid. For the grid, one can use another Smolyak parameter, L^G, usually larger than L_B. In this work, we always use $L^G = L^B + 1$.

Using the standard Smolyak algorithm to tackle a quantum system, s, interacting weakly with a quantum environment or bath, b, leads to poor convergence of the energy-level transitions. Indeed, in the standard approach, the *same* Smolyak parameter, L, is used for both system and bath parts. This is shown in the blue curves (•) of Fig.2 on a test with five H_2 modes and a water clathrate cage described using three normal modes. This originates from the restriction $\mathscr{R}(\boldsymbol{\ell})$, leading to some basis functions describing the bath modes (clathrate cage) being present in the ground state expansion, but not in the excited states of the system (H_2), see supplement for a typical example.[35] This imbalanced description of the ground state and the excited state levels leads to a lack of couplings in these excited states. This worsens as the bath is described using a growing number of DoF, leading to a large deviation in the energy transition. Increasing the value of L can gradually reduce the importance of the missing coupling basis functions, which is the origin of the slow convergence of the transitions as a function of L.

The problem can also be attenuated by introducing a system-bath separation scheme, given the relatively weak coupling between the system and bath, affording an accurate description of the system part and a mild description of the bath part. Specifically, different Smolyak parameters, L_s and L_b, are assigned to the system and bath parts, respectively. However, the convergence issue persists. To solve the problem and ensure the full coupling

of the system and bath (full-coupling SSBS), we introduce here an extra parameter L_m covering the entire system with $L_m{=}L_s{+}L_b$, i.e. a direct-product between the system basis functions and the bath ones. This modification leads to a fast convergence of the energy-level transitions as shown in the black lines ($\times$) in Fig.2, which, however, requires a relatively large number of basis functions. In order to better converge the lower states, we can further relax the condition on L_m ($L_m{=}L_s{+}L_b$) to $L_s{\leq}L_m{\leq}L_s{+}L_b$, which finalizes the constraints (equivalent to $\mathscr{R}(\boldsymbol{\ell})$) for general SBSS as

$$\mathscr{R}^{SSBS}(\boldsymbol{\ell}) : \begin{cases} |\boldsymbol{\ell}_s| \leq L_s \\ |\boldsymbol{\ell}_b| \leq L_b \\ |\boldsymbol{\ell}| \leq L_m \\ L_s + L_b \geq L_m \geq L_s \geq L_b, \end{cases} \tag{5}$$

where $|\boldsymbol{\ell}_s|{=}\sum_{i=1}^{n^s} \ell_i^s$ and $|\boldsymbol{\ell}_b|{=}\sum_{i=1}^{n^b} \ell_i^b$. It is worth noting that $|\boldsymbol{\ell}|{=}|\boldsymbol{\ell}_s|{+}|\boldsymbol{\ell}_b|$. The coefficient $D_{\boldsymbol{\ell}}$ in Eq.(4) is now obtained numerically by a direct expansion from the original Smolyak method.[16,35] The accuracy in describing the bath and system-bath coupling can be simply controlled by adjusting L_b and L_m, respectively. SSBS is equivalent to the original Smolyak scheme when $L_m{=}L_s{=}L_b$. An illustration of SSBS is shown in Fig.1.

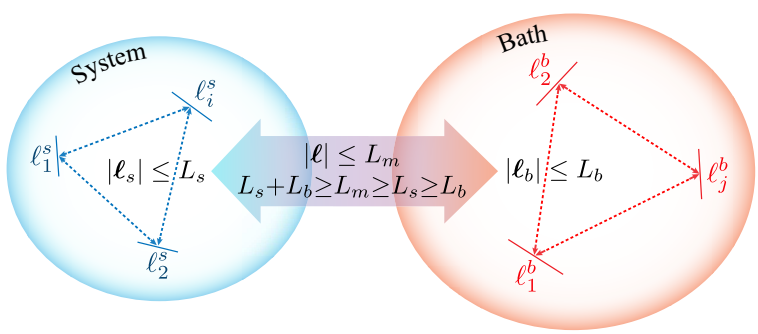

Figure 1: (color online) An illustration of SSBS. The arrows denote the couplings between different modes (the solid lines) in the system and bath. The Smolyak terms in the system and bath are restricted by $|\boldsymbol{\ell}_s| \leq L_s$ and $|\boldsymbol{\ell}_b| \leq L_b$, respectively, while they are restricted overall by L_m to ensure the system-bath coupling. See the text for more details.

SSBS improves the convergence of the system part independently from the convergence of the bath part. Introducing L_m guarantees the presence of "necessary" basis functions for different states and so ensures a fast convergence of the energy-level transitions without a full convergence of the states. Thus it enables usage of a smaller basis set with respect to the original Smolyak scheme, as a smaller L can be used. Various combinations of L_m, L_s, and L_b can be chosen, according to the considered molecules, in which the full-coupling SSBS is one of the extreme cases (see the supplement[35]). A moderate combination, balancing the system-bath coupling and efficiency, is $C^0_{L_m}$: L_s=L_m-1, L_b=$\lceil L_m/2 \rceil$ ($\lceil\ \rceil$ denotes the ceiling function).

3 Results and discussion

As an application of SSBS, we consider a hydrogen molecule in a 5^{12} sII clathrate hydrate cage.[30,32] Numerous studies have contributed to the related quantum simulation,[25,34,36–39] usually considering the cage to be rigid, namely, a quantum particle trapped within a confining potential. According to the radial distribution of the oxygen atom from the cage center, the first three shells of sII cage contain 20, 20, and 36 water molecules, respectively.[24,38] In this work, only the first two shells are taken into account since the effects of the third shell are relatively weak.[24,34] The water molecules in the second layer are assumed to be rigid to constrain the first layer in a solid phase environment. The dynamics of the water molecules in the inner layer is taken into account and described using fully delocalized rectilinear normal modes (first set). Thus the full dimension of the cage is 180 (9 per water molecule), where the 60 translational and 60 rotational DoF are crucial. As usual, the normal modes are sorted in terms of increasing frequencies, associated with the translation, rotation, bending, and stretching motions. The H_2 molecule is described by three translational DoF and two spherical angles. Furthermore, it is considered rigid, with a fixed inter-nuclear bond length[25] at the equilibrium geometry of H_2 in the cage. The full Hamiltonian (H_2 and the first water

layer) is given in the supplement.[35] In terms of basis set, one-dimensional harmonic oscillator basis sets (HO) with $N_{\ell_i}^{b_i}$=1+$B_i\ell_i$ are associated with the NM of the cage and also to the 3 translational coordinates of H_2. Then, to describe H_2 rotations, we use a spherical harmonics basis (Y_j^m, with j_{max}=$B_i\ell_i$, $N_{\ell_i}^{b_i}$=$(1+B_i\ell_i)^2$) that can describe both ortho- and para- H_2.[24,34] For the grid points, we use Gauss-Hermite quadrature for the HO basis set and Lebedev grid points for the spherical spherical harmonics basis. The potential energy surface (PES) considered is constructed using the flexible water-water SPC/Fw potential[40] (one body and pair contributions) and the water-hydrogen SPC/E potential.[41] The initial locations and orientations of the H_2O molecules are optimized by minimizing the H_2-cage interaction energy. The Cartesian atomic positions of the reference cage and the analytical expression of the full potential are given in the supplement.[35]

We present in Table 1 the number of required basis functions in SSBS ($N_{L_m}^{SSBS}$) when considering different DoF of the cage for the C_4^0 scheme: L_m=4, L_s=3, L_b=2 (note here L_m^G=5) and B_s=B_b=2. For H_2, the B_i of the spherical harmonics basis is set equal to that of HO for convenience (they can be different generally). The results are compared with those of full-coupling SSBS, direct-product scheme N_{L_s,L_b}^{dp}=$\prod_{i=1}^{n_s}(N_{L_s}^{b_i})\prod_{i=1}^{n_b}(N_{L_b}^{b_i})$ and standard Smolyak algorithm $N_{L_m}^s$. Since the same basis function can be present in several Smolyak terms, $N_{L_m}^{SSBS}$ and $N_{L_m}^s$ can technically be made even smaller by removing the duplication.[35] We should note, for the Smolyak method, that the L_m chosen here is actually far too small to obtain full convergence.

Table 1: Number of basis functions required when considering caged H_2 with different DoF of the cage in conventional direct-product scheme (N_{L_s,L_b}^{dp}), standard Smolyak algorithm (N^s), SSBS with scheme $C_{L_m}^0$ ($N_{L_m}^{SSBS}$) at L_m=4, L_m^G=5 and the related full-coupling SSBS.

C_4^0	N_{L_s,L_b}^{dp}	$N_{L_m}^s$	$N_{L_m}^{SSBS}$	$N_{\text{full coupling}}^{SSBS}$
(L_m,L_s,L_b)	/	(4,4,4)	(4,3,2)	(5,3,2)
5+3D	2100875	122740	104580	347034
5+60D	1.5×10^{46}	2624892199	179516184	1003272294
5+120D	1.2×10^{88}	65600962720	1365782634	7732041654

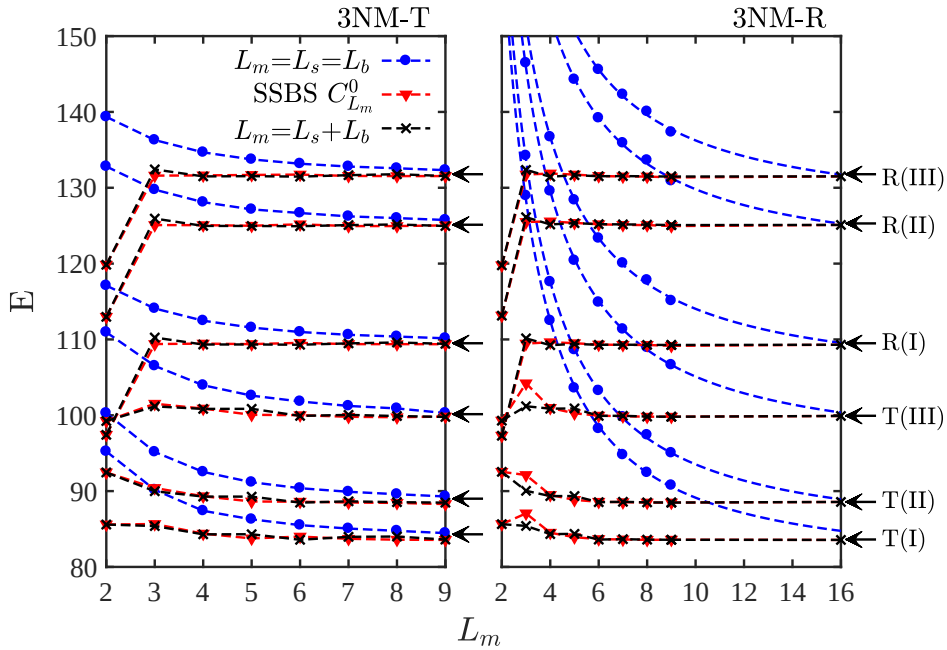

Figure 2: (color online) The convergence of TR states of H_2 as a function of L_m in standard Smolyak algorithm (blue •) and SSBS $C^0_{L_m}$ at B_s=B_b=2 (red ▼) as indicated. The results of full-coupling SSBS (black ×) are also shown for a comparison. The benchmark results of direct-product scheme are marked with black arrows (←). The dashed lines are guide for the eyes. The test is performed for 3 NM involving mainly translational (3NM-T) or rotational (3NM-R) DoF of H_2O molecules to ensure the convergence in general.

The SSBS simulation is performed with our program ElVibRot,[22,42,43] a Smolyak method quantum simulation package working with curvilinear coordinates. The diagonalization is performed with a block-Davidson procedure. It has been verified in a series of quantum simulations.[22–25,34] As an application of our SSBS approach, we present in Fig.2 convergence tests for an H_2 clathrate hydrate, considering 3 NM of the cage associated mainly with the translational (3NM–T) or rotational (3NM–R) water DoF. The tests are performed at B_s=B_b=2 as a function of L_m for different constraints $\mathscr{R}^{SSBS}(\boldsymbol{\ell})$ to cover the behaviour of different combinations. The results shown in Fig.2 for $C^0_{L_m}$ and full-coupling SSBS are also compared with those of a standard Smolyak algorithm and a direct-product scheme. More details can be found in the supplement.[35]

With the standard Smolyak algorithm (blue dashed line in Fig.2), the transition energy levels show a very slow convergence as a function of L_m. This convergence issue is even

worse when the rotational NM of water (3NM–R) are considered. In this case, the standard Smolyak results have to be extrapolated to convergence. When aiming at converged TR transitions of H_2, a large portion of basis functions is not only "wasted" for a rigorous description of the cage part, but also causes the deviation of the energies of TR states as mentioned above. Therefore, at least L_m=9 is required to converge the TR states of H_2 with a standard Smolyak method for the 3NM–T model, leading to N_9^s=74387784 basis functions. SSBS overcomes this problem for the TR transitions, exhibiting very fast convergence with L_m. All the tested combinations show similar robust convergence. This suggests that the actual L_m required for a fair tensor compression with Smolyak method for TR transitions is smaller than expected. Indeed, L_m=4 seems sufficient (see Table 1). These convergence properties hold when more NM are taken into account. Therefore, it is possible to achieve simulations of much larger systems.

By increasing the number of NM in the simulation with SSBS ($C_{L_m}^0$) until convergence (around 100 NM, see the blue dashed curves in Fig.3(a)), we obtain the TR transitions of H_2, denoted as T(I, II, III) and R(I, II, III), respectively. The results for rigid cage, with 60 and 120 NM obtained at C_4^0 are shown in Table 2 (named 60NM and 120NM, respectively). The convergence of each simulation is confirmed by increasing the L_m in $C_{L_m}^0$. The splitting of TR levels, ΔT=T(III)-T(I) and ΔR=R(III)-R(I), are also shown as a reference. The simulation time for 120 NM is around 7.8 hours in parallel computation on 15 nodes with 80 cores per node. The results are compared with the experimental data and typical previous simulation results,[24,44] in which the Ref[44] used the same SPC/E potential as this work but different cage configurations. The results obtained in Ref[24] accounted for the quantum effects of the overall rotation of the water molecules with an adiabatic-QDMC approach and they show a weak effect on the transition energies with respect to a rigid cage. Overall, our TR energies obtained agree well with the experiment, reproducing the triplet splittings of TR states. The T(III) and R(I) states have very good agreement with the experiment. However, ΔT and ΔR are under- and over-estimated, respectively. The deviation is likely due to the PES used

in our simulation.[45,46]

Furthermore, we observe in Table 2 that the published calculation using a rigid cage[44] is in better agreement with the experimental data than our current calculations, even with a rigid cage (first line of Table 2), although both calculations use the same water-hydrogen SPC/E potential.[41] This effect is due to the shape of the water cage which is different between the two studies. Indeed, to compute the normal modes, the water positions of the first shell have been optimized. More generally, we can argue that such difference is coming from the full potential (water-hydrogen and water-water contributions) which is not perfect. Our current approach is able to consider explicitly the large number of degrees of freedom and therefore to probe directly the quality of a potential.

Table 2: The energies (in cm^{-1}) of TR transitions, obtained with SSBS at C_4^0, with rigid cage, 60 or 120 delocalized normal modes (named 60NM and 120NM). The results of the calculation considering localized normal modes, $60T_{H_2O}$, $60R_{H_2O}$ and full 120 $(T+R)_{H_2O}$ dynamics are also shown. They are compared with those of experiment and typical previous works.[24,44]

	T(I)	T(II)	T(III)	R(I)	R(II)	R(III)	ΔT	ΔR
rigid	83.6	88.5	99.8	109.3	125.0	131.5	16.3	22.3
60NM	**86.1**	**90.9**	**102.3**	**110.1**	**125.5**	**132.1**	**16.1**	**22.0**
120NM	**86.7**	**91.6**	**102.9**	**110.8**	**125.0**	**132.0**	**16.2**	**21.2**
$60T_{H_2O}$	85.9	90.4	102.1	110.3	125.3	132.1	16.2	21.8
$60R_{H_2O}$	84.9	89.7	101.1	111.3	125.4	132.4	16.2	21.1
$\mathbf{120(T+R)_{H_2O}}$	**86.4**	**91.3**	**102.8**	**111.2**	**125.3**	**132.4**	**16.3**	**21.2**
exp.	71.0	80.2	101.1	110.0	116.5	122.1	30.1	12.1
Ref.[44]	74.5	74.7	97.5	109.0	119.4	128.1	23.1	19.2
Ref.[24]	80.5	85.1	107.7	108.6	117.8	124.1	27.2	15.5

Specifically, the fair reproduction of TR transitions with the rigid cage model suggests that we have obtained suitable initial H_2O locations through our geometry optimization. With 60 and 120 NM, the ΔT, ΔR, and R levels are not observably influenced by H_2O dynamics, as was the case for other simulations,[24] while the T levels are overall lifted by roughly 3 cm^{-1}. In Fig.3(a) we show the T(I) and T(III) transitions as a function of NM ranging from 0 (rigid cage) to 120 DoF. The increase of T energies slows down around 70

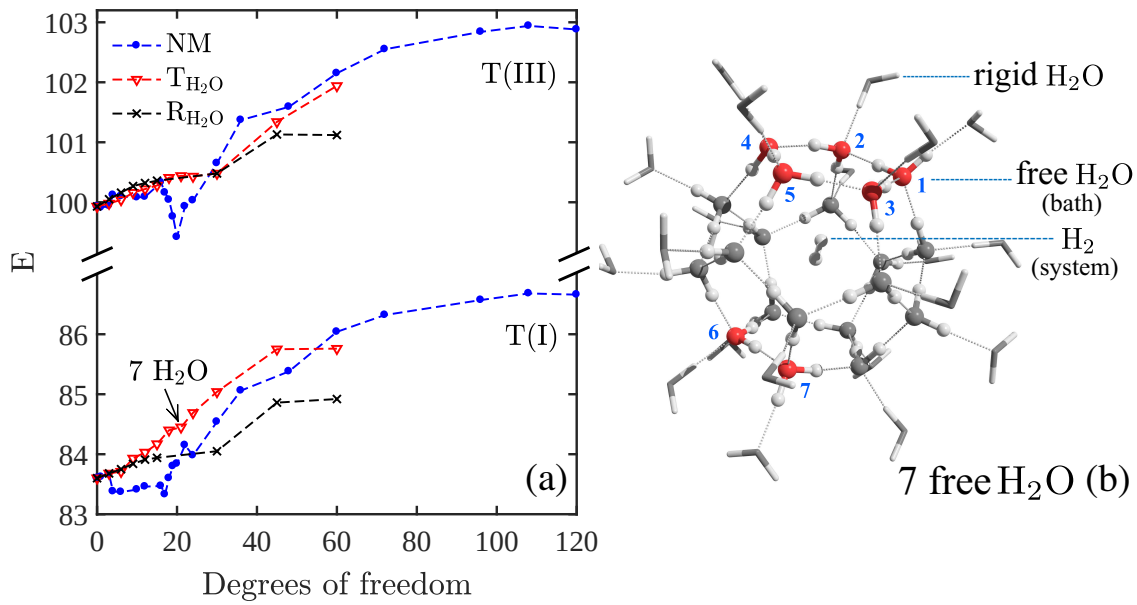

Figure 3: (color online) Panel (a) shows the T(I) and T(III) energies as a function of number of DoF for the delocalized NM (first set), T_{H_2O}, or R_{H_2O} modes (second set). Panel (b) shows the initial locations of the first 7 H_2O molecules chosen (colored) for T_{H_2O} and R_{H_2O} as indicated in panel (a).

NM, reaching convergence already around 100 NM. When examining the full energy levels of H_2 clathrate hydrate, we found that the coupling of the excitation of H_2 with that of NM forms a series of states around the TR levels. For instance, the coupling of T(I) with the excitation of NM forms several levels between R(I) and R(II). Besides, the convergence of R levels only requires just a few basis functions. It indicates an almost free rotation of H_2 in the cage.

Instead of the delocalized normal modes employed above, we could use another set (the second set) of normal modes localized around water molecules. Those modes are sorted in terms of increasing frequencies for each water molecule, but, one has some freedom to select the water molecule ordering. Therefore, the first few H_2O are chosen in the same cage pentagon as shown in Fig.3(b) (see the supplement[35] for the full selection). They are named, respectively, T_{H_2O}, R_{H_2O} and $(T+R)_{H_2O}$ when rotation or translation or both motions is taken into account (see Table 2 and Fig.3). The TR transition energies at $60T_{H_2O}$, $60R_{H_2O}$ and full $120(T+R)_{H_2O}$ obtained at C_4^0 are shown in Table 2. The results of $60T_{H_2O}$

and 120(T+R)$_{H_2O}$ are very close to those of 60NM and 120NM as expected, since the first 120 NM mainly consist of 60 translational and 60 rotational DoF. It suggests that couplings in the cage are correctly taken into account. This further confirms the convergence of our simulation.

4 Conclusion

In conclusion, we have proposed an SSBS method to address the TR transitions of H_2 molecule in an sII clathrate hydrate cage considering the cage dynamics. In terms of system-bath separation, this Smolyak algorithm method overcomes the issues with eigenstate convergence and provides rapid convergence for the transitions of the "system" part without converging the "bath" part transitions. It significantly pushes the limit of the Smolyak algorithm to over a hundred DoF for some molecules. The obtained results agree well with experimental data. The simulations performed in this work use small-scale computing capabilities, implying that SSBS can be extended to even more DoF when deployed on large-scale architectures. By using $L_m > L_s = L_b$ in Eq.(5), this method is generally helpful for dealing with similar convergence issues when using the Smolyak algorithm in quantum simulations.

In terms of applications, the proposed Smolyak scheme, SBBS, is well-adapted to study a molecule coupled to an environment. The present work shows this for weak couplings but we plan to extend to system-bath systems that show stronger couplings. Atoms or molecules in fullerenes,[4,47–49] carbon nanotubes,[50,51] clathrate (aluminosilicates),[52] metal-organic frameworks[53] are all accessible with this new approach. For more complex systems involving several molecules encapsulated in a nanoscale environment, the calculations are formally doable. However, the size of the basis set might be very large and possibly require some adjustments or coupling of the Smolyak scheme for the bath to other approaches for the system, like the one used to study two H_2 molecules in hydrate clathrate.[54]

Acknowledgement

A.C. acknowledges the funding support from E-CAM European Centre of Excellence, European Union's Horizon 2020 research and innovation program under Grant No. 676531. We acknowledges the computational resource of the *styx* in Institut de Chimie Physique, Université Paris-Saclay, the *mandelbrot* in Maison de la Simulation, CEA-Saclay, and the *JUWELS* in Jülich Supercomputing Centre provided by Dr. Alan O'Cais in E-CAM.

Supporting Information Available

- Supplement_SSBS.pdf: additional details on the Smolyak algorithm, SSBS, and the setup and test of the simulation.

This information is available free of charge via the Internet at http://pubs.acs.org

References

(1) Cram, D. J.; Cram, J. M. Host-Guest Chemistry. *Science* **1974**, *183*, 803–809.

(2) Lehn, J.-M. Supramolecular Chemistry: Receptors, Catalysts, and Carriers. *Science* **1985**, *227*, 849–856.

(3) Stucky, G. D.; Mac Dougall, J. E. Quantum Confinement and Host/Guest Chemistry: Probing a New Dimension. *Science* **1990**, *247*, 669–678.

(4) Valdés, Á.; Carrillo-Bohórquez, O.; Prosmiti, R. Fully Coupled Quantum Treatment of Nanoconfined Systems: A Water Molecule Inside a Fullerene C_{60}. *J. Chem. Theory Comput.* **2018**, *14*, 6521–6531.

(5) Rotter, I.; Bird, J. P. A Review of Progress in the Physics of Open Quantum Systems: Theory and Experiment. *Rep. Prog. Phys.* **2015**, *78*, 114001.

(6) de Vega, I.; Alonso, D. Dynamics of Non-Markovian Open Quantum Systems. *Rev. Mod. Phys.* **2017**, *89*, 015001.

(7) Weimer, H.; Kshetrimayum, A.; Orús, R. Simulation Methods for Open Quantum Many-Body Systems. *Rev. Mod. Phys.* **2021**, *93*, 015008.

(8) Soley, M. B.; Bergold, P.; Gorodetsky, A. A.; Batista, V. S. Functional Tensor-Train Chebyshev Method for Multidimensional Quantum Dynamics Simulations. *J. Chem. Theory Comput.* **2022**, *18*, 25–36.

(9) Alvermann, A.; Fehske, H. Sparse Polynomial Space Approach to Dissipative Quantum Systems: Application to the Sub-Ohmic Spin-Boson Model. *Phys. Rev. Lett.* **2009**, *102*, 150601.

(10) Bonfanti, M.; Martinazzo, R. In *Research Advances in Quantum Dynamics*; Bracken, P., Ed.; IntechOpen: Rijeka, 2016; Chapter 8.

(11) Strathearn, A.; Kirton, P.; Kilda, D.; Keeling, J.; Lovett, B. W. Efficient Non-Markovian Quantum Dynamics Using Time-Evolving Matrix Product Operators. *Nat. Commun.* **2018**, *9*, 3322.

(12) Beck, M.; Jäckle, A.; Worth, G.; Meyer, H.-D. The Multiconfiguration Time-Dependent Hartree (MCTDH) Method: A Highly Efficient Algorithm for Propagating Wavepackets. *Phys. Rep.* **2000**, *324*, 1–105.

(13) Meyer, H.-D.; Gatti, F.; Worth, G. A. In *Multidimensional Quantum Dynamics*; Meyer, H.-D., Gatti, F., Worth, G. A., Eds.; John Wiley & Sons, Ltd: Chichester, West-Sussex, United Kingdom, 2009; Chapter 1, pp 1–7.

(14) Richings, G.; Polyak, I.; Spinlove, K.; Worth, G.; Burghardt, I.; Lasorne, B. Quantum Dynamics Simulations Using Gaussian Wavepackets: The vMCG Method. *Int. Rev. Phys. Chem.* **2015**, *34*, 269–308.

(15) Bonfanti, M.; Worth, G. A.; Burghardt, I. In *Quantum Chemistry and Dynamics of Excited States*; González, L., Lindh, R., Eds.; John Wiley & Sons, Ltd: Chichester, West-Sussex, United Kingdom, 2020; Chapter 12, pp 383–411.

(16) Smolyak, S. A. Quadrature and Interpolation Formulas for Tensor Products of Certain Classes of Functions. *Dokl. Akad. Nauk SSSR* **1963**, *148*, 1042–1045.

(17) Gradinaru, V. Strang Splitting for the Time-Dependent Schrödinger Equation on Sparse Grids. *SIAM J. Numer. Anal.* **2008**, *46*, 103–123.

(18) Lasser, C.; Lubich, C. Computing Quantum Dynamics in the Semiclassical Regime. *Acta Numer.* **2020**, *29*, 229–401.

(19) Avila, G.; Carrington, T. Nonproduct Quadrature Grids for Solving the Vibrational Schrödinger Equation. *J. Chem. Phys.* **2009**, *131*, 174103.

(20) Avila, G.; Carrington, T. Using Nonproduct Quadrature Grids to Solve the Vibrational Schrödinger Equation in 12D. *J. Chem. Phys.* **2011**, *134*, 054126.

(21) Avila, G.; Carrington, T. A Multi-Dimensional Smolyak Collocation Method in Curvilinear Coordinates for Computing Vibrational Spectra. *J. Chem. Phys.* **2015**, *143*, 214108.

(22) Lauvergnat, D.; Nauts, A. Torsional Energy Levels of Nitric Acid in Reduced and Full Dimensionality with ElVibRot and Tnum. *Phys. Chem. Chem. Phys.* **2010**, *12*, 8405–8412.

(23) Lauvergnat, D.; Nauts, A. Quantum Dynamics with Sparse Grids: A Combination of Smolyak Scheme and Cubature. Application to Methanol in Full Dimensionality. *Spectrochim. Acta A Mol. Biomol. Spectrosc.* **2014**, *119*, 18 – 25.

(24) Benoit, D. M.; Lauvergnat, D.; Scribano, Y. Does Cage Quantum Delocalisation Influence the Translation–Rotational Bound States of Molecular Hydrogen in Clathrate Hydrate? *Faraday Discuss.* **2018**, *212*, 533–546.

(25) Lauvergnat, D.; Felker, P.; Scribano, Y.; Benoit, D. M.; Bačić, Z. H_2, HD, and D_2 in the Small Cage of Structure II Clathrate Hydrate: Vibrational Frequency Shifts from Fully Coupled Quantum Six-Dimensional Calculations of the Vibration-Translation-Rotation Eigenstates. *J. Chem. Phys.* **2019**, *150*, 154303.

(26) Avila, G.; Mátyus, E. Toward Breaking the Curse of Dimensionality in (Ro)Vibrational Computations of Molecular Systems with Multiple Large-Amplitude Motions. *J. Chem. Phys.* **2019**, *150*, 174107.

(27) Avila, G.; Matyus, E. Full-dimensional (12D) Variational Vibrational States of $CH_4{\cdot}F^-$: Interplay of Anharmonicity and Tunneling. *J. Chem. Phys.* **2019**, *151*, 154301.

(28) Avila, G.; Papp, D.; Czakó, G.; Mátyus, E. Exact Quantum Dynamics Background of Dispersion Interactions: Case Study for $CH_4{\cdot}Ar$ in Full (12) Dimensions. *Phys. Chem. Chem. Phys.* **2020**, *22*, 2792–2802.

(29) Schüth, F. Hydrogen and Hydrates. *Nature* **2005**, *434*, 712–713.

(30) Mao, W. L.; Mao, H.-k.; Goncharov, A. F.; Struzhkin, V. V.; Guo, Q.; Hu, J.; Shu, J.; Hemley, R. J.; Somayazulu, M.; Zhao, Y. Hydrogen Clusters in Clathrate Hydrate. *Science* **2002**, *297*, 2247–2249.

(31) Lee, H.; Lee, J.-w.; Kim, D. Y.; Park, J.; Seo, Y.-T.; Zeng, H.; Moudrakovski, I. L.; Ratcliffe, C. I.; Ripmeester, J. A. Tuning Clathrate Hydrates for Hydrogen Storage. *Nature* **2005**, *434*, 743–746.

(32) Ulivi, L.; Celli, M.; Giannasi, A.; Ramirez-Cuesta, A. J.; Bull, D. J.; Zoppi, M. Quantum

Rattling of Molecular Hydrogen in Clathrate Hydrate Nanocavities. *Phys. Rev. B* **2007**, *76*, 161401(R).

(33) Xu, M.; Elmatad, Y. S.; Sebastianelli, F.; Moskowitz, J. W.; Bačić, Z. Hydrogen Molecule in the Small Dodecahedral Cage of a Clathrate Hydrate: Quantum Five-Dimensional Calculations of the Coupled Translation-Rotation Eigenstates. *J. Phys. Chem. B* **2006**, *110*, 24806–24811.

(34) Powers, A.; Scribano, Y.; Lauvergnat, D.; Mebe, E.; Benoit, D. M.; Bačić, Z. The Effect of the Condensed-Phase Environment on the Vibrational Frequency Shift of a Hydrogen Molecule inside Clathrate Hydrates. *J. Chem. Phys.* **2018**, *148*, 144304.

(35) See Supplemental Material for more details on the Smolyak algorithm, SSBS, and the setup and test of the simulation.

(36) Colognesi, D.; Celli, M.; Ulivi, L.; Xu, M.; Bačić, Z. Neutron Scattering Measurements and Computation of the Quantum Dynamics of Hydrogen Molecules Trapped in the Small and Large Cages of Clathrate Hydrates. *J. Phys. Chem. A* **2013**, *117*, 7314–7326.

(37) Celli, M.; Powers, A.; Colognesi, D.; Xu, M.; Bačić, Z.; Ulivi, L. Experimental Inelastic Neutron Scattering Spectrum of Hydrogen Hexagonal Clathrate-Hydrate Compared with Rigorous Quantum Simulations. *J. Chem. Phys.* **2013**, *139*, 164507.

(38) Powers, A.; Marsalek, O.; Xu, M.; Ulivi, L.; Colognesi, D.; Tuckerman, M. E.; Bačić, Z. Impact of the Condensed-Phase Environment on the Translation–Rotation Eigenstates and Spectra of a Hydrogen Molecule in Clathrate Hydrates. *J. Phys. Chem. Lett.* **2016**, *7*, 308–313.

(39) Schmidt, M.; Millar, J.; Roy, P.-N. Path Integral Simulations of Confined Parahydrogen Molecules Within Clathrate Hydrates: Merging Low Temperature Dynamics with the Zero-Temperature Limit. *J. Chem. Phys.* **2022**, *156*, 014303.

(40) Wu, Y.; Tepper, H. L.; Voth, G. A. Flexible Simple Point-Charge Water Model with Improved Liquid-State Properties. *J. Chem. Phys.* **2006**, *124*, 024503.

(41) Alavi, S.; Ripmeester, J. A.; Klug, D. D. Molecular-Dynamics Study of Structure II Hydrogen Clathrates. *J. Chem. Phys.* **2005**, *123*, 024507.

(42) Lauvergnat, D. ElVibRot-TnumTana. `https://github.com/lauvergn/ElVibRot-TnumTana` (accessed March 25, 2022).

(43) Chen, A.; Nauts, A.; Lauvergnat, D. ElVibRot-MPI: Parallel Quantum Dynamics with Smolyak Algorithm for General Molecular Simulation. 2021, arXiv:2111.13655. arXiv.org ePrint archive. `https://arxiv.org/abs/2111.13655` (accessed March 25, 2022).

(44) Xu, M.; Sebastianelli, F.; Bačić, Z. Quantum Dynamics of H_2, D_2, and HD in the Small Dodecahedral Cage of Clathrate Hydrate: Evaluating H_2-Water Nanocage Interaction Potentials by Comparison of Theory with Inelastic Neutron Scattering Experiments. *J. Chem. Phys.* **2008**, *128*, 244715.

(45) Homayoon, Z.; Conte, R.; Qu, C.; Bowman, J. M. Full-Dimensional, High-Level Ab Initio Potential Energy Surfaces for $H_2(H_2O)$ and $H_2(H_2O)_2$ with Application to Hydrogen Clathrate Hydrates. *J. Chem. Phys.* **2015**, *143*, 084302.

(46) Valiron, P.; Wernli, M.; Faure, A.; Wiesenfeld, L.; Rist, C.; Kedžuch, S.; Noga, J. R12-calibrated H_2O-H_2 Interaction: Full Dimensional and Vibrationally Averaged Potential Energy Surfaces. *J. Chem. Phys.* **2008**, *129*, 134306.

(47) Felker, P. M.; Bačić, Z. Communication: Quantum Six-Dimensional Calculations of the Coupled Translation-Rotation Eigenstates of $H_2O@C_{60}$. *J. Chem. Phys.* **2016**, *144*, 201101.

(48) Carrillo-Bohórquez, O.; Valdés, Á.; Prosmiti, R. Encapsulation of a Water Molecule Inside C_{60} Fullerene: The Impact of Confinement on Quantum Features. *J. Chem. Theory Comput.* **2021**, *17*, 5839–5848.

(49) Xu, M.; Felker, P. M.; Bačić, Z. H_2O Inside the Fullerene C_{60}: Inelastic Neutron Scattering Spectrum from Rigorous Quantum Calculations. *J. Chem. Phys.* **2022**, *156*, 124101.

(50) Mondelo-Martell, M.; Huarte-Larrañaga, F. Competition of Quantum Effects in H_2/D_2 Sieving in Narrow Single-Wall Carbon Nanotubes. *Mol. Phys.* **2021**, *119*, e1942277.

(51) de Lara-Castells, M. P.; Mitrushchenkov, A. O. Mini Review: Quantum Confinement of Atomic and Molecular Clusters in Carbon Nanotubes. *Front. Chem.* **2021**, *9*, 796890.

(52) Zhong, J.-Q.; Wang, M.; Akter, N.; Kestell, J. D.; Niu, T.; Boscoboinik, A. M.; Kim, T.; Stacchiola, D. J.; Wu, Q.; Lu, D.; Boscoboinik, J. A. Ionization-Facilitated Formation of 2D (Alumino)Silicate–Noble Gas Clathrate Compounds. *Adv. Funct. Mater.* **2019**, *29*, 1806583.

(53) FitzGerald, S. A.; Allen, K.; Landerman, P.; Hopkins, J.; Matters, J.; Myers, R.; Rowsell, J. L. C. Quantum Dynamics of Adsorbed H_2 in the Microporous Framework MOF-5 Analyzed Using Diffuse Reflectance Infrared Spectroscopy. *Phys. Rev. B* **2008**, *77*, 224301.

(54) Felker, P. M.; Lauvergnat, D.; Scribano, Y.; Benoit, D. M.; Bačić, Z. Intramolecular Stretching Vibrational States and Frequency Shifts of $(H_2)_2$ Confined Inside the Large Cage of Clathrate Hydrate from an Eight-Dimensional Quantum Treatment Using Small Basis Sets. *J. Chem. Phys.* **2019**, *151*, 124311.
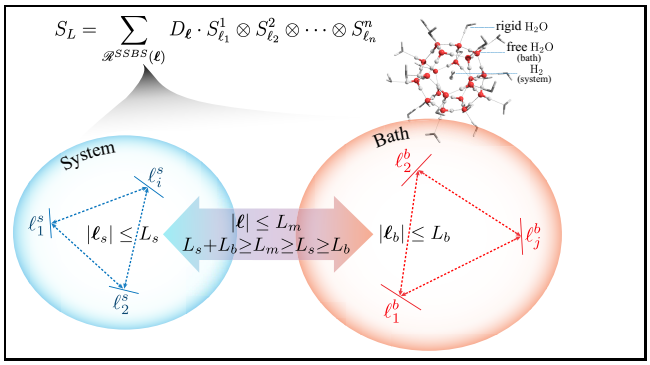
Graphical TOC Entry